

Semiparametric Copula Estimation for Spatially Correlated Multivariate Mixed Outcomes: Analyzing Visual Sightings of Fin Whales from Line Transect Survey

Tomotaka Momozaki¹, Tomoyuki Nakagawa², Shonosuke Sugasawa³
and Hiroko Kato Solvang⁴

¹Department of Information Sciences, Tokyo University of Science

²School of Data Science, Meisei University

³Faculty of Economics, Keio University

⁴Marine Mammals Research Group, Institute of Marine Research

Abstract

Multivariate data having both continuous and discrete variables is known as mixed outcomes and has widely appeared in a variety of fields such as ecology, epidemiology, and climatology. In order to understand the probability structure of multivariate data, the estimation of the dependence structure among mixed outcomes is very important. However, when location information is equipped with multivariate data, the spatial correlation should be adequately taken into account; otherwise, the estimation of the dependence structure would be severely biased. To solve this issue, we propose a semiparametric Bayesian inference for the dependence structure among mixed outcomes while eliminating spatial correlation. To this end, we consider a hierarchical spatial model based on the rank likelihood and a latent multivariate Gaussian process. We develop an efficient algorithm for computing the posterior using the Markov Chain Monte Carlo. We also provide a scalable implementation of the model using the nearest-neighbor Gaussian process under large spatial datasets. We conduct a simulation study to validate our proposed procedure and demonstrate that the procedure successfully accounts for spatial correlation and correctly infers the dependence structure among outcomes. Furthermore, the procedure is applied

to a real example collected during an international synoptic krill survey in the Scotia Sea of the Antarctic Peninsula, which includes sighting data of fin whales (*Balaenoptera physalus*), and the relevant oceanographic data.

Key words: Dependence modeling; Extended rank likelihood; Quasi-posterior; Gaussian process; Markov Chain Monte Carlo

1 Introduction

Many marine ecosystems are characterized by several levels of interactions between marine species such as populations of fish, birds, sea mammals etc. and the marine environment (Mann and Lazier, 2005). Understanding the nature of these interactions is imperative because they define ecosystem functioning, and provide insight into the effect of climate change on the dynamics of the marine ecosystems (Tett et al., 2013). The data for investigating these interactions are usually obtained by scientific survey and the outcome summarized abiotic and biotic observations mixes several continuous (e.g., acoustic registration, biomass, abundance) and discrete (e.g., counted data, sighted data) numerical number. In addition, the data are spatially and temporally correlated. Therefore, it faces a statistical challenge to accurately estimate the interactions among marine species and environmental factors in the marine ecosystem using the data.

For modeling the interactions among variables, there are a lot of statistical methods such as factor analysis and principle component analysis (e.g. Manly and Alberto, 2016), graphical modeling (e.g. Jordan, 2004) and copulas (e.g. Joe, 2014). In particular, copulas are known to be attractive tools for explicitly modeling dependence structures without modeling marginal distributions, and can also be successfully applied even when outcomes are mixed (i.e. outcomes include both continuous and discrete variables). As techniques for estimating copula, Hoff (2007) proposed the extended rank likelihood for parametric copulas and developed a simple Gibbs sampler for Bayesian inference on copulas. While these methods are quite useful for modeling the dependence structure, the multivariate observations are assumed to be independent each other. However, beginning with the example of marine ecosystems mentioned above, in many applications such as in epidemi-

ology, climatology, medicine, and sociology, multivariate data with location information are often available, and spatial correlation must be appropriately taken into account; otherwise, the estimation of the dependence structure among outcomes could be severely biased.

To demonstrate the potential effects of spatial correlation in the dependence modeling, we consider a simulated multivariate data with 300 samples and 4 mixed outcomes, where the detailed settings are explained in Section 4. Figure 1 shows the estimation results of the method of Hoff (2007) (denoted by BGC) applied to the simulated data. It is observed that 95% credible intervals of BGC do not include most of the true values, indicating that the inference of the dependence structure is severely biased without taking spatial correlation into account. On the other hand, the 95% credible intervals based on our proposed method (denoted by spBGC), presented in Section 3, can suitably capture the true correlation. Thus, in multivariate data equipped with location information, it is essential to take the spatial correlation into account adequately in order to make correct inference on the dependence structure.

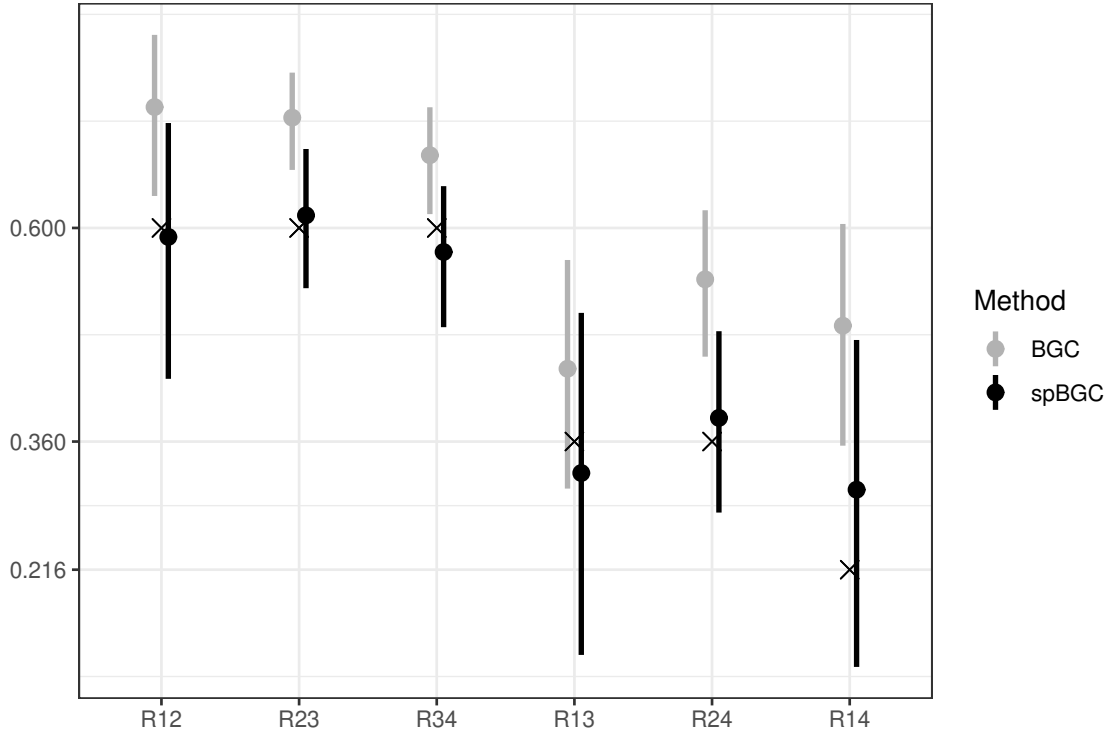


Figure 1: The 95% credible interval and the posterior median of each correlation coefficient by Hoff (2007)'s (BGC) and our proposed methods (spBGC): cross marks denote true values.

Our proposal is to use a spatially-correlated hierarchical model combined with the extended rank likelihood (Hoff, 2007) for semiparametric Bayesian inference on copulas. We develop an efficient algorithm for computing the posteriors of the dependence structure and the spatial range parameter using the Markov Chain Monte Carlo. We also provide a scalable implementation of the model using the nearest-neighbor Gaussian process (Datta et al., 2016) under large spatial datasets. We conduct a simulation study to validate our proposed procedure and demonstrate that the procedure successfully accounts for spatial correlation and correctly infers the dependence structure among outcomes. Remarkably, as the spatial correlation becomes stronger among observations, our proposed method outperforms Hoff (2007)’s one not taking into account spatial correlation. Furthermore, our proposed procedure is applied to a real example collected during an international synoptic krill survey in the Scotia Sea of the Antarctic Peninsula, which includes sighting data of fin whales (*Balaenoptera physalus*), and the relevant oceanographic data (Macaulay et al., 2019; Krafft et al., 2019).

As related works in spatial modeling, there are a number of works on modeling multivariate spatial data. For example, Dey et al. (2022) and Krock et al. (2023) propose efficient modeling (relatively high-dimensional) multivariate spatial data for Gaussian outcomes, and Feng and Dean (2012) and Torabi (2014) consider multivariate models based on generalized linear mixed models. Furthermore, there are attempts to use copula in multivariate spatial modeling such as Musfer et al. (2017), Krupskii et al. (2018), Krupskii and Genton (2019) and Gong and Huser (2022) to mention a few. Since the above methods consider joint estimation of both marginal and dependence structures, one may lose efficiency of estimation by a large number of nuisance parameters in the marginal distributions and the estimation of the dependence could be biased due to potential specifications of the marginal distributions. Hence, it would be more reasonable to directly modeling the dependence structure like the proposed method.

The rest of this paper is organized as follows. Section 2 introduces the extended rank likelihood and the semiparametric Bayesian inference for the dependence structure proposed by Hoff (2007). Section 3 proposes a semiparametric Bayesian inference for the dependence structure in spatially correlated mixed outcomes and develops an efficient algorithm for computing the posterior using the Markov Chain Monte Carlo (MCMC).

The algorithm is extended to be more scalable implementation using the nearest-neighbor Gaussian process even under large spatial datasets. Section 4 shows the simulation results, including a comparison with the method of Hoff (2007), to validate the usefulness of our proposed method. Section 5 presents an application of our proposed method using real data collected during an international synoptic krill survey in the Scotia Sea of the Antarctic Peninsula. Section 6 provides the conclusion and some remarks. The R code implementing the proposed method is available at GitHub repository (<https://github.com/t-momozaki/spBGC>).

2 Extended rank likelihood for semiparametric copula estimation

Suppose we observe p -dimensional observations of mixed outcomes $\mathbf{y}_i = (y_{i1}, \dots, y_{ip})^\top$ for $i = 1, 2, \dots, n$, where each variable could be variety of types of outcomes such as continuous, count and ordered variables. Here, we are interested in the dependence structure among p outcomes. The marginal distributions of each component in \mathbf{y}_i are not of interest and are nuisance parameters in Hoff (2007)'s and our framework. Let \mathbf{z}_i be a p -dimensional continuous latent variable for \mathbf{y}_i and we consider the following Gaussian copula model.

$$\begin{aligned} \mathbf{z} = (\mathbf{z}_1^\top, \mathbf{z}_2^\top, \dots, \mathbf{z}_n^\top)^\top &\sim N_{pn}(\mathbf{0}, \mathbf{I}_n \otimes \mathbf{R}), \\ y_{ij} &= F_j^{-1}[\Phi(z_{ij})], \end{aligned} \tag{1}$$

where \mathbf{R} is the $p \times p$ correlation matrix and \mathbf{I}_n , \otimes , each F_j^{-1} , and $\Phi(\cdot)$ denote the $n \times n$ identity matrix, the Kronecker product, the inverse of an unknown univariate cumulative distribution function, and the cumulative distribution function of the standard Normal distribution, respectively. Here we are interested in the correlation matrix \mathbf{R} for the dependence structure. For this model, Hoff (2007) defined the following extended rank likelihood.

$$L(\mathbf{R}) = \Pr(\mathbf{z} \in D | \mathbf{R}) = \int_D \phi_{pn}(\mathbf{z}; \mathbf{0}, \mathbf{I}_n \otimes \mathbf{R}) d\mathbf{z}, \tag{2}$$

where $\phi_k(\mathbf{x}; \boldsymbol{\mu}, \boldsymbol{\Sigma})$ be the k -dimensional multivariate normal density with mean vector $\boldsymbol{\mu}$ and variance-covariance matrix $\boldsymbol{\Sigma}$. Observing $\mathbf{y} = (\mathbf{y}_1^\top, \mathbf{y}_2^\top, \dots, \mathbf{y}_n^\top)^\top$ provides us infor-

mation that \mathbf{z} must lie in the set

$$D = \{\mathbf{z} \in \mathbb{R}^{pm} : \max(z_{kj} : y_{kj} < y_{ij}) < z_{ij} < \min(z_{kj} : y_{ij} < y_{kj})\}$$

since F_j is a nondecreasing function and observing $y_{ij} < y_{i'j}$ for any $i \neq i'$ implies that $z_{ij} < z_{i'j}$. Note that this likelihood depends only on the parameter of interest, \mathbf{R} , and not on the nuisance parameters, $\mathbf{F} = (F_1, F_2, \dots, F_p)^\top$. It can be regarded as a kind of marginal likelihood in the presence of nuisance parameters and derived in terms of the decomposition theorem on sufficient statistics. That is,

$$\begin{aligned} p(\mathbf{y}|\mathbf{R}, \mathbf{F}) &= p(\mathbf{z} \in D, \mathbf{y}|\mathbf{R}, \mathbf{R}) \\ &= \Pr(\mathbf{z} \in D|\mathbf{R})p(\mathbf{y}|\mathbf{z} \in D, \mathbf{R}, \mathbf{F}) \end{aligned}$$

and then to estimate \mathbf{R} , it is sufficient to use only $\Pr(\mathbf{z} \in D|\mathbf{R})$. The function (2) is called the extended rank likelihood since it is derived from the marginal probability of the ranks and can be seen as a multivariate version of the rank likelihood (Pettitt, 1982; Heller and Qin, 2001) and is free for the nuisance parameters for continuous and discrete data.

Hoff (2007) further developed an algorithm for computing the posterior of \mathbf{R} using the Gibbs sampler with the parameter expansion technique (Liu and Wu, 1999). The algorithm can also be used when observations are missing at random. We can easily implement the algorithm in the R programming language using the `sbgcop.mcmc` function of the `sbgcop` package.

3 Copula estimation under spatial correlation

3.1 Latent models with spatial correlation

Suppose we observe observations of mixed outcomes $\mathbf{y}_{\mathcal{S}}$ equipped with location information \mathcal{S} , where $\mathbf{y}_{\mathcal{S}} = (\mathbf{y}(\mathbf{s}_1)^\top, \mathbf{y}(\mathbf{s}_2)^\top, \dots, \mathbf{y}(\mathbf{s}_n)^\top)^\top$, $\mathbf{y}(\mathbf{s}_i) = (y_1(\mathbf{s}_i), y_2(\mathbf{s}_i), \dots, y_p(\mathbf{s}_i))^\top$, $\mathcal{S} = \{\mathbf{s}_1, \mathbf{s}_2, \dots, \mathbf{s}_n\}$, and \mathbf{s}_i denotes typically a two-dimensional vector of longitude and latitude. These observations are characterized by spatial dependence and correlation such that nearby observations have similar properties. In such data, spatial correlation should be adequately taken into account, or else the estimation of the dependence structure among

outcomes would be severely biased. Therefore we consider a hierarchical spatial model and a latent multivariate Gaussian process. We define the following “spatial Gaussian copula”, a Gaussian copula model to take into account spatial correlation.

$$\mathbf{z}_S = (\mathbf{z}(\mathbf{s}_1)^\top, \mathbf{z}(\mathbf{s}_2)^\top, \dots, \mathbf{z}(\mathbf{s}_n)^\top)^\top \sim N_{pn}(\mathbf{0}, \mathbf{H}(\phi) \otimes \mathbf{R}), \quad (3)$$

where $\mathbf{z}(\mathbf{s}_i)$ denotes a latent variable equipped with location information \mathbf{s}_i and $\mathbf{H}(\phi)$ is a $n \times n$ matrix whose (i, i') -element is a valid correlation function $\rho(\|\mathbf{s}_i - \mathbf{s}_{i'}\|; \phi)$ with spatial range parameter ϕ such as exponential correlation function $\rho(\|\mathbf{s}_i - \mathbf{s}_{i'}\|; \phi) = \exp(-\|\mathbf{s}_i - \mathbf{s}_{i'}\|/\phi)$. The $\mathbf{H}(\phi)$ is also interpreted as the correlation matrix of $\mathbf{z}_{(j)}^S = (z_j(\mathbf{s}_1), z_j(\mathbf{s}_2), \dots, z_j(\mathbf{s}_n))^\top$ with $\text{Corr}(z_j(\mathbf{s}_i), z_j(\mathbf{s}_{i'})) = \rho(\|\mathbf{s}_i - \mathbf{s}_{i'}\|; \phi)$. Hereafter, we write $\mathbf{H}(\phi)$ as \mathbf{H} , the dependence on ϕ being implicit, with similar notation for all spatial correlation matrices. Note that the spatial Gaussian copula is the same as a multivariate Gaussian process with correlation structure

$$\text{Corr}(\mathbf{z}(\mathbf{s}_i), \mathbf{z}(\mathbf{s}_{i'})) = \rho(\|\mathbf{s}_i - \mathbf{s}_{i'}\|; \phi) \cdot \mathbf{R},$$

and its correlation structure is known as separable correlation (e.g. Chapter 9 in [Banerjee et al., 2003](#)).

We consider the extended rank likelihood for the inference of the dependence structure in spatially correlated mixed outcomes, i.e., the correlation matrix \mathbf{R} in the spatial Gaussian copula. The observation \mathbf{y}_S provides us information about the latent variable \mathbf{z}_S such that for $j = 1, 2, \dots, p$, $z_j(\mathbf{s}_i) < z_j(\mathbf{s}_{i'})$ holds when $y_j(\mathbf{s}_i) < y_j(\mathbf{s}_{i'})$ for arbitrary pair $z_j(\mathbf{s}_i)$ and $z_j(\mathbf{s}_{i'})$ with $i \neq i'$, i.e., $\mathbf{z}_{(j)}^S$ must lie in the set

$$D_j = \{\mathbf{z}_{(j)}^S \in \mathbb{R}^n : \max[z_j(\mathbf{s}_k) : y_j(\mathbf{s}_k) < y_j(\mathbf{s}_i)] < z_j(\mathbf{s}_i) < \min[z_j(\mathbf{s}_k) : y_j(\mathbf{s}_i) < y_j(\mathbf{s}_k)]\}.$$

Then, the extended rank likelihood of \mathbf{R} including the spatial range parameter ϕ under the spatial Gaussian copula is given by

$$L(\mathbf{R}, \phi) = \int_{D_1} \int_{D_2} \cdots \int_{D_p} \phi_{pn}(\mathbf{z}_S; \mathbf{0}, \mathbf{H} \otimes \mathbf{R}) d\mathbf{z}_S. \quad (4)$$

Note that this extended rank likelihood takes into account the spatially varying ranks that are not captured by the likelihood in Hoff (2007).

3.2 Posterior computation

The extended rank likelihood (4) allows us to develop an effective algorithm for computing the posteriors of \mathbf{R} and ϕ using the MCMC. The joint posterior of \mathbf{R} and ϕ , $\mathbf{z}_{\mathcal{S}}$ given $\mathbf{y}_{\mathcal{S}}$ can be expressed as follows by using the extended rank likelihood (4).

$$p(\mathbf{R}, \phi, \mathbf{z}_{\mathcal{S}} | \mathbf{y}_{\mathcal{S}}) \propto p(\mathbf{R})p(\phi)\phi_{np}(\mathbf{z}_{\mathcal{S}}; \mathbf{0}, \mathbf{H} \otimes \mathbf{R}), \quad \mathbf{z}_{\mathcal{S}} \in D_1 \times D_2 \times \cdots \times D_p. \quad (5)$$

As for the prior distribution of \mathbf{R} , we consider the semi-conjugate prior in the Gaussian copula model as in Hoff (2007). That is, let \mathbf{V} follow the inverse-Wishart prior distribution, $IW(v_0, v_0 \mathbf{V}_0)$ and use the fact that \mathbf{R} is equal to the distribution of the correlation matrix where each element is $\mathbf{V}_{ij} / \sqrt{\mathbf{V}_i \mathbf{V}_j}$. The MCMC algorithm to generate posterior samples of \mathbf{R} , ϕ , and $\mathbf{z}(\mathbf{s}_i)$ for $i = 1, 2, \dots, n$ is provided as follows.

- (Sampling of $\mathbf{z}(\mathbf{s}_i)$) Generate $\mathbf{z}(\mathbf{s}_i)$ from a p -dimensional truncated normal distribution, $TN_p(\boldsymbol{\mu}_{\mathbf{s}_i}, \boldsymbol{\Sigma}_{\mathbf{s}_i}; \boldsymbol{\ell}, \mathbf{u})$, where

$$\boldsymbol{\mu}_{\mathbf{s}_i} = (\mathbf{H}_{\mathbf{s}_i, \mathcal{S}_{-i}} \mathbf{H}_{\mathcal{S}_{-i}}^{-1} \otimes \mathbf{I}_p) \mathbf{z}_{\mathcal{S}_{-i}}, \quad \boldsymbol{\Sigma}_{\mathbf{s}_i} = (1 - \mathbf{H}_{\mathbf{s}_i, \mathcal{S}_{-i}} \mathbf{H}_{\mathcal{S}_{-i}}^{-1} \mathbf{H}_{\mathbf{s}_i, \mathcal{S}_{-i}}^{\top}) \mathbf{R},$$

$\mathcal{S}_{-i} = \{\mathbf{s}_{i'} | i' \neq i, i' \in \mathbb{N}\}$, $\mathbf{H}_{\mathbf{s}_i, \mathcal{S}_{-i}}$ is the $(n-1)$ -dimensional cross-correlation row vector between the $\mathbf{z}(\mathbf{s}_i)$ and $\mathbf{z}_{\mathcal{S}_{-i}}$, $\mathbf{H}_{\mathcal{S}_{-i}}$ is the $(n-1) \times (n-1)$ correlation matrix of $\mathbf{z}_{\mathcal{S}_{-i}}$, and the j -th element of p -dimensional vectors $\boldsymbol{\ell}$ and \mathbf{u} are

$$\ell_j = \max[z_j(\mathbf{s}_k) : y_j(\mathbf{s}_k) < y_j(\mathbf{s}_i)] \quad \text{and} \quad u_j = \min[z_j(\mathbf{s}_k) : y_j(\mathbf{s}_i) < y_j(\mathbf{s}_k)],$$

denoting the lower and upper bounds of the truncated normal distribution in each dimension.

- (Sampling \mathbf{R}) Generate \mathbf{V} from $IW(v_0 + n, v_0 \mathbf{V}_0 + \sum_{i=1}^n h_i^{-1} [\mathbf{z}(\mathbf{s}_i) - \bar{\mathbf{z}}_i][\mathbf{z}(\mathbf{s}_i) - \bar{\mathbf{z}}_i]^{\top})$, where

$$h_i = 1 - \mathbf{H}_{\mathbf{s}_i, \mathcal{C}_i} \mathbf{H}_{\mathcal{C}_i}^{-1} \mathbf{H}_{\mathbf{s}_i, \mathcal{C}_i}^{\top}, \quad \bar{\mathbf{z}}_i = (\mathbf{H}_{\mathbf{s}_i, \mathcal{C}_i} \mathbf{H}_{\mathcal{C}_i}^{-1} \otimes \mathbf{I}_p) \mathbf{z}_{\mathcal{C}_i},$$

$\mathcal{C}_i = \{\mathbf{s}_{i'} | i' < i, i' \in \mathbb{N}\}$, $\mathbf{H}_{\mathbf{s}_i, \mathcal{C}_i}$ is the c_i -dimensional cross-correlation row vector between the $\mathbf{z}(\mathbf{s}_i)$ and $\mathbf{z}_{\mathcal{C}_i}$ with $c_i = |\mathcal{C}_i|$, and $\mathbf{H}_{\mathcal{C}_i}$ is the $c_i \times c_i$ correlation matrix of $\mathbf{z}_{\mathcal{C}_i}$, and transform $\mathbf{R}_{ij} = \mathbf{V}_{ij} / \sqrt{\mathbf{V}_i \mathbf{V}_j}$.

- (Sampling ϕ) The full conditional of ϕ is proportional to

$$|\mathbf{H}|^{-p/2} \exp \left\{ -\frac{1}{2} \sum_{i=1}^n h_i^{-1} [\mathbf{z}(\mathbf{s}_i) - \bar{\mathbf{z}}_i]^\top \mathbf{R}^{-1} [\mathbf{z}(\mathbf{s}_i) - \bar{\mathbf{z}}_i] \right\}$$

A random-walk Metropolis-Hastings is used to sample from this distribution.

3.3 Scalable posterior computation under large spatial data

The proposed inference procedure introduced in the previous section has to compute the inverse of the $(n-1) \times (n-1)$ matrix in generating $\mathbf{z}(\mathbf{s}_i)$, \mathbf{R} , and ϕ , which is a computationally cost $O[(n-1)^3]$ and requires a large amount of time when the sample size n is large. To address this problem, we employ the nearest-neighbor Gaussian process (Datta et al., 2016) for $\mathbf{z}_{\mathcal{S}}$ that uses a multivariate normal distribution with a sparse precision matrix, defined as

$$p(\mathbf{z}_{\mathcal{S}}) = \prod_{i=1}^n \phi_p(\mathbf{z}(\mathbf{s}_i); \mathbf{B}_{\mathbf{s}_i, \mathcal{N}_i}, F_{\mathbf{s}_i} \mathbf{R}),$$

where

$$\mathbf{B}_{\mathbf{s}_i} = \mathbf{H}_{\mathbf{s}_i, \mathcal{N}_i} \mathbf{H}_{\mathcal{N}_i}^{-1} \otimes \mathbf{I}_p, \quad F_{\mathbf{s}_i} = 1 - \mathbf{H}_{\mathbf{s}_i, \mathcal{N}_i} \mathbf{H}_{\mathcal{N}_i}^{-1} \mathbf{H}_{\mathbf{s}_i, \mathcal{N}_i}^\top,$$

$\mathcal{N}_i = \{\mathbf{s}_{i'} | i' \text{ is an index of } m\text{-nearest neighbor of } \mathbf{s}_i\}$, $\mathbf{H}_{\mathbf{s}_i, \mathcal{N}_i}$ is the n_i -dimensional cross-correlation row vector between the $\mathbf{z}(\mathbf{s}_i)$ and $\mathbf{z}_{\mathcal{N}_i}$ with $n_i = |\mathcal{N}_i| (\leq m)$, and $\mathbf{H}_{\mathcal{N}_i}$ is the $n_i \times n_i$ correlation matrix of $\mathbf{z}_{\mathcal{N}_i}$.

Under the nearest-neighbor Gaussian process for $\mathbf{z}_{\mathcal{S}}$, the full conditional distribution of $\mathbf{z}(\mathbf{s}_i)$ can be expressed as

$$p(\mathbf{z}(\mathbf{s}_i) | \mathbf{z}_{\mathcal{S}_{-i}}) = p(\mathbf{z}(\mathbf{s}_i) | \mathbf{z}_{\mathcal{D}_i}),$$

where $\mathcal{D}_i = \{\mathbf{s}_{i'} | \mathbf{s}_i \in \mathcal{N}_{i'}\} \cup \mathcal{N}_i$ since $(\mathbf{z}(\mathbf{s}_i), \mathbf{z}_{\mathcal{D}_i}) \perp\!\!\!\perp \mathbf{z}_{\mathcal{S}_{-i} \setminus \mathcal{D}_i}$. Therefore, the MCMC algorithm for generating posterior samples of \mathbf{R} , ϕ , and $\mathbf{z}(\mathbf{s}_i)$ using the nearest-neighbor Gaussian process is provided as follows.

- (Sampling of $\mathbf{z}(\mathbf{s}_i)$) Generate $\mathbf{z}(\mathbf{s}_i)$ from a p -dimensional truncated normal distribution, $TN_p(\tilde{\boldsymbol{\mu}}_{\mathbf{s}_i}, \tilde{\boldsymbol{\Sigma}}_{\mathbf{s}_i}; \boldsymbol{\ell}, \mathbf{u})$, where

$$\tilde{\boldsymbol{\mu}}_{\mathbf{s}_i} = (\mathbf{H}_{\mathbf{s}_i, \mathcal{D}_i} \mathbf{H}_{\mathcal{D}_i}^{-1} \otimes \mathbf{I}_p) \mathbf{z}_{\mathcal{D}_i}, \quad \tilde{\boldsymbol{\Sigma}}_{\mathbf{s}_i} = (1 - \mathbf{H}_{\mathbf{s}_i, \mathcal{D}_i} \mathbf{H}_{\mathcal{D}_i}^{-1} \mathbf{H}_{\mathbf{s}_i, \mathcal{D}_i}^\top) \mathbf{R},$$

$\mathbf{H}_{\mathbf{s}_i, \mathcal{D}_i}$ is the d_i -dimensional cross-correlation row vector between the $\mathbf{z}(\mathbf{s}_i)$ and $\mathbf{z}_{\mathcal{D}_i}$ with $d_i = |\mathcal{D}_i|$, $\mathbf{H}_{\mathcal{D}_i}$ is the $d_i \times d_i$ correlation matrix of $\mathbf{z}_{\mathcal{D}_i}$.

- (Sampling \mathbf{R}) Generate \mathbf{V} from

$$IW \left(v_0 + n, v_0 \mathbf{V}_0 + \sum_{i=1}^n F_{\mathbf{s}_i}^{-1} [\mathbf{z}(\mathbf{s}_i) - \mathbf{B}_{\mathbf{s}_i} \mathbf{z}_{\mathcal{N}_i}] [\mathbf{z}(\mathbf{s}_i) - \mathbf{B}_{\mathbf{s}_i} \mathbf{z}_{\mathcal{N}_i}]^\top \right),$$

and transform $\mathbf{R}_{ij} = \mathbf{V}_{ij} / \sqrt{\mathbf{V}_i \mathbf{V}_j}$.

- (Sampling ϕ) The full conditional of ϕ is proportional to

$$|\mathbf{H}|^{-p/2} \exp \left\{ -\frac{1}{2} \sum_{i=1}^n F_{\mathbf{s}_i}^{-1} [\mathbf{z}(\mathbf{s}_i) - \mathbf{B}_{\mathbf{s}_i} \mathbf{z}_{\mathcal{N}_i}]^\top \mathbf{R}^{-1} [\mathbf{z}(\mathbf{s}_i) - \mathbf{B}_{\mathbf{s}_i} \mathbf{z}_{\mathcal{N}_i}] \right\}$$

A random-walk Metropolis-Hastings is used to sample from this distribution.

The computation of $\tilde{\boldsymbol{\mu}}_{\mathbf{s}_i}$ and $\tilde{\boldsymbol{\Sigma}}_{\mathbf{s}_i}$ in the full conditional distribution of $\mathbf{z}(\mathbf{s}_i)$ with the nearest-neighbor Gaussian process requires at most only $d_i \times d_i$ ($d_i < (n-1)$), rather than the $(n-1) \times (n-1)$ matrix calculation required by the MCMC algorithm of Section 3 with the full Gaussian process. It also requires only $m \times m$ matrix calculations in \mathbf{R} and ϕ . Hence, the computational cost is reduced from the original cost $O[(n-1)^3]$ to $O(d_i^3)$ in generating the posterior sample of $\mathbf{z}(\mathbf{s}_i)$, and is greatly reduced to $O(m^3)$ in generating the posterior samples of \mathbf{R} and ϕ , since m can be set to a small value (e.g., $m = 5$ or 10).

4 Simulation study

This section demonstrates through a simulation study that our proposed approach successfully accounts for spatial correlation and correctly infers the dependence structure among the spatially correlated multivariate mixed outcomes including a comparison with Hoff (2007)'s one. To this end, We consider the spatial Gaussian copula (3) with $n =$

50, 100, 300 and $p = 6, 9$ where $\phi = 0.05, 0.25, 0.5$ and $\mathbf{R}_{12} = 0.5$, $\mathbf{R}_{14} = 0.3$, $\mathbf{R}_{15} = 0.2$, $\mathbf{R}_{23} = -0.2$, $\mathbf{R}_{24} = -0.3$, $\mathbf{R}_{35} = 0.4$, $\mathbf{R}_{45} = -0.5$, and all others to zero for $j < j'$. The location information s_{i1} and s_{i2} are generated from $\text{Unif}(-2, 2)$. Under the spatial Gaussian copula, we generate a simulated dataset based on [Smith \(2021\)](#):

Step 1. Calculate the spatial correlation matrix \mathbf{H} with location information $\mathbf{s}_i = (s_{i1}, s_{i2})^\top$.

Step 2. Generate latent variables \mathbf{z}_S from the multivariate Gaussian process (3).

Step 3. Calculate $y_j(\mathbf{s}_i) = F_j^{-1}[\Phi(z_j(\mathbf{s}_i))]$, where F_j is a specified cumulative distribution function for $j = 1, 2, \dots, p$.

In our simulation setting, $y_1(\mathbf{s}_i) \sim \text{Bernoulli}(0.5)$, $y_2(\mathbf{s}_i) \sim \text{Poi}(15)$, $y_3(\mathbf{s}_i) \sim \text{Poi}(5)$, $y_4(\mathbf{s}_i) \sim \text{OrderedCategorical}(0.3, 0.15, 0.1, 0.25, 0.2)$, and all other $y_j(\mathbf{s}_i)$ s are generated from normal distributions.

For the simulated dataset, we apply our proposed and [Hoff \(2007\)](#) methods, denoted by spBGC and BGC, respectively. In doing so, we use 2000 draws for the posterior computation after discarding the first 1000 draws as burn-in using an $IW(p + 2, (p + 2)\mathbf{I})$ prior for \mathbf{V} . We compute posterior medians as point estimates of $\mathbf{R}_{jj'}$ for $j < j'$ and evaluate their performance with mean squared error (MSE) defined as $q^{-1} \sum_{j < j'} \mathbf{R}_{jj'}$ where $q = p(p - 1)/2$. We also compute 95% credible intervals and calculate coverage probability (CP) defined as $q^{-1} \sum_{j < j'} I(\mathbf{R}_{jj'} \in \text{CI}_{jj'})$ where $I(\cdot)$ is the indicator function and $\text{CI}_{jj'}$ is the 95% credible interval of $\mathbf{R}_{jj'}$. These values are averaged over 300 replications of simulated datasets.

Figure 2 shows boxplots of MSE. When there is little spatial correlation ($\phi = 0.05$), i.e., when the observations are almost independent, the proposed (spBGC) and [Hoff \(2007\)](#)'s (BGC) methods are comparable. However, as the spatial correlation becomes stronger, the performance of BGC gets worse compared with our spBGC. For interval estimation, Table 1 presents the results for CP. For little spatial correlation, the CPs of both BGC and spBGC are around the nominal level. For stronger spatial correlation, the CP of our spBGC is relatively stable at the nominal level, whereas the CP of BGC is far below the level. Remarkably, when $n = 300$ and $\phi = 0.5$, the difference of CP of BGC from the nominal level is about 5 times lower for $p = 6$ and about 9 times lower for $p = 9$ than that of our spBGC.

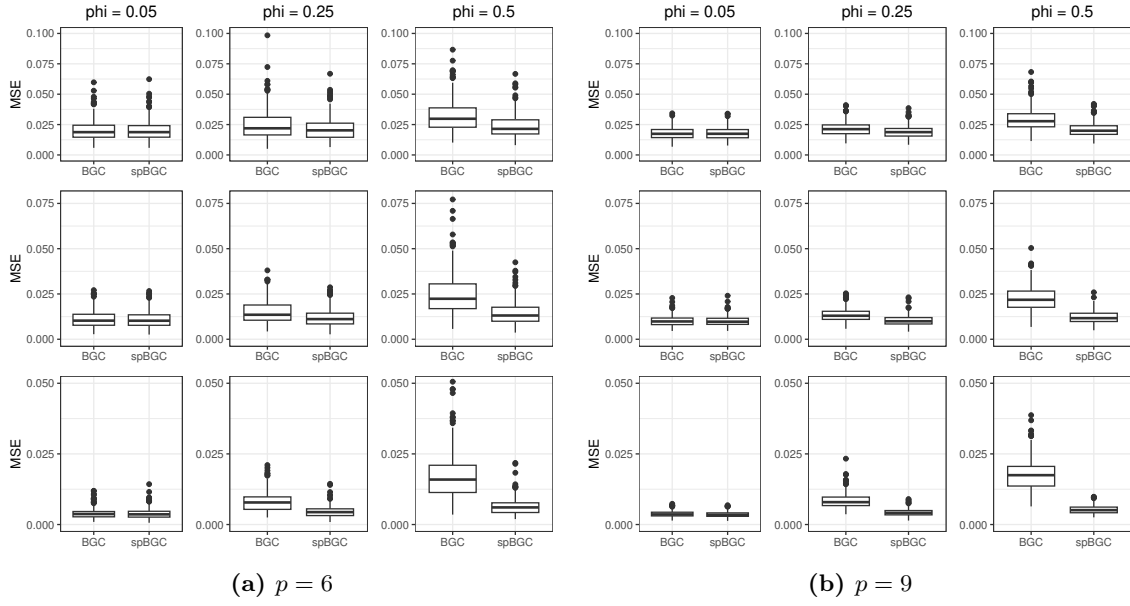


Figure 2: Boxplots of MSE based on 300 replications: upper row for $n = 50$, middle row for $n = 100$, lower row for $n = 300$.

Table 1: CP of 95% credible intervals averaged over 300 replications.

	(a) $p = 6$			(b) $p = 9$		
	$\phi = 0.05$	$\phi = 0.25$	$\phi = 0.5$	$\phi = 0.05$	$\phi = 0.25$	$\phi = 0.5$
$n = 50$				$n = 50$		
spBGC	0.959	0.951	0.949	spBGC	0.965	0.961
BGC	0.958	0.936	0.891	BGC	0.965	0.948
$n = 100$				$n = 100$		
spBGC	0.946	0.942	0.923	spBGC	0.957	0.953
BGC	0.948	0.904	0.806	BGC	0.956	0.914
$n = 300$				$n = 300$		
spBGC	0.944	0.928	0.884	spBGC	0.951	0.936
BGC	0.937	0.810	0.634	BGC	0.948	0.794

5 Real data applications

We applied our method to visual sightings of fin whales from line transect surveys in the Southern Ocean. Visual observations were carried out onboard three of the six vessels

participating in the 2019 krill survey: the R/V Kronprins Haakon (KPH), the F/V Cabo de Hornos (CDH), and the RRS Discovery (DIS). Surveys covered the periods 10 Jan - 22 Feb (KPH), 09 Jan - 11 Mar (CDH) and 03 Jan - 11 Feb (DIS). Observations were taken by dedicated observers, in sea states below Force 6, and generally covered all daylight hours (continuously modified to follow local time and daylength depending on latitude and longitude). On the CDH, only one dedicated observer was present onboard, while two and four dedicated observers were present on the KPH and DIS, respectively. This resulted in a reduced effort especially on the CDH 3 compared to the DIS. To alleviate the problem of under-staffing, dedicated observations on CDH and KPH were generally limited to one forward quadrant (port side, or 270°-360° degrees on the KPH, starboard side, or 0°-90° on the CDH, relative to the bow of the vessel), with observations in other quadrants recorded as “incidental sightings.” On the CDH and KPH, observations were carried out from inside the bridge or an inside observation deck, and sightings were taken as voice recordings directly to disc, using the system developed for the Norwegian surveys for North Atlantic minke whales (Øien, 1995). This system allows the dedicated observer to record effort, weather, and sightings through a handheld microphone, while maintaining full visual attention. Observations on the DIS were carried out from outside platforms by two dedicated observers and one data recorder. Data were entered into the Logger software system (<http://www.marineconservationresearch.co.uk/downloads/logger-2000-rainbowclick-software-downloads/>). Standard variables were recorded, including estimated radial distance, angle relative to the vessel’s heading, species, group size, swimming direction, and initial cue. The radial distance was estimated using either 7 × 50 reticulated binoculars or (on the KPH) 30-cm equidistant steps on a mast ladder positioned 16.6 meters forward of the observation deck. These steps correspond to different angles of depression relative to the horizon, calibrated for the height of each observer. Essentially, this method follows the exact same logic as that of reticulated binoculars or a distance stick. Angle relative to the bow was determined using a standard angle board. Weather and sea-state were recorded every 15-30 minutes, and in some cases (KPH) detailed weather station data were available from the ship’s automatic data recording system. The sighting data of fin whales was taken as counted data. In addition, we included surface temperature (Celsius) and water depth (meter) for a 1-nm segment to

investigate the association from environmental data for the biological community. Figure xx gives spatial plots for krill biomass (Krill), sighting data of fin whales (Whale), surface temperature (SST), depth data (Depth), slope for the depth (Slope), and gradient surface temperature (SST.grd). Brighter/darker dots' colors of surface temperature and water depth mean higher/lower temperature and shallower/deeper water depth, respectively. Data on water depth came from the ETOPO 1 bathymetric dataset available at <https://www.ncei.noaa.gov/products/etopo-global-relief-model>. Data were extracted for the middle position of each 1-nm segment throughout the survey tracks. Data on sea surface temperature SST were obtained from the OISST dataset available at <https://www.ncei.noaa.gov/products/optimum-interpolation-sst> and extracted in the same way as for depth data. The slope for the depth is the maximum rate of change in the depth from that cell to its neighbors calculated by the Slope tool of the Surface toolset in ArcGIS (<https://desktop.arcgis.com/en/arcmap/10.3/tools/spatial-analyst-toolbox/an-overview-of-the-surface-tools.htm>). The lower the slope value, the flatter the terrain; the higher the slope value, the steeper the terrain. The gradient surface temperature is also calculated by Slope applied to SST.

We are interested in the dependence structure of the krill biomass and sighting data of fin whales and that of each of these outcomes and environmental factors (SST, Depth, Slope, and SST.grd). Thus, thereafter, this application focuses on the posterior inference of these dependence structures. We compare results of our proposed method (spBGC) with that of Hoff (2007)'s one (BGC) not taking account into spatial correlation. Before the comparison, we check mixing properties of our spBGC. Using an $IW(p+2, (p+2)\mathbf{I})$ prior, i.e., $IW(8, 8\mathbf{I})$ for \mathbf{V} , we use 2000 draws for the posterior computation after discarding the first 1000 draws as burn-in. Figure 4 shows mixing and autocorrelation results of our interest correlation coefficients, respectively. As can be seen from these figures, the mixing properties of our spBGC algorithm are quite satisfactory, that is, convergence to stationarity appears, and the autocorrelation at lag-20 is quite close to zero for most elements.

Based on 2000 posterior draws, we compute posterior medians and 95% credible intervals of the correlation coefficients, which are shown in Figure 5 and Tables 2 and 3. It is observed that our spBGC and BGC provide quite different results in some correlation

coefficients. In particular, based on their credible intervals, spBGC shows that Krill has no significant positive (or negative) one with outcomes other than Whale, and Whale with those other than Krill and SST, while the credible intervals of BGC do not contain zero for all outcomes in Krill, and for other than Depth in Whale. This implies that BGC may have overestimated the positive (or negative) correlation coefficients among outcomes by not taking into account spatial correlation among observations.

As a dependence structure among outcomes, one may be interested in the conditional independence in addition to the correlation coefficients. Figure 5 and Tables 2 and 3 also present the results of partial correlations. We can see that these results, as well as the correlation coefficients, are quite different between spBGC and BGC. The credible intervals of spBGC do not contain zero only for the partial correlation between Krill and Whale, while those of BGC contain zero for some partial correlations. Although we do not display here, the results of these partial correlations allow us to draw a graph consisting of nodes for outcomes and edges for the conditional dependency. This facilitates to visually interpret the dependence structure of multivariate data with a large number of outcomes.

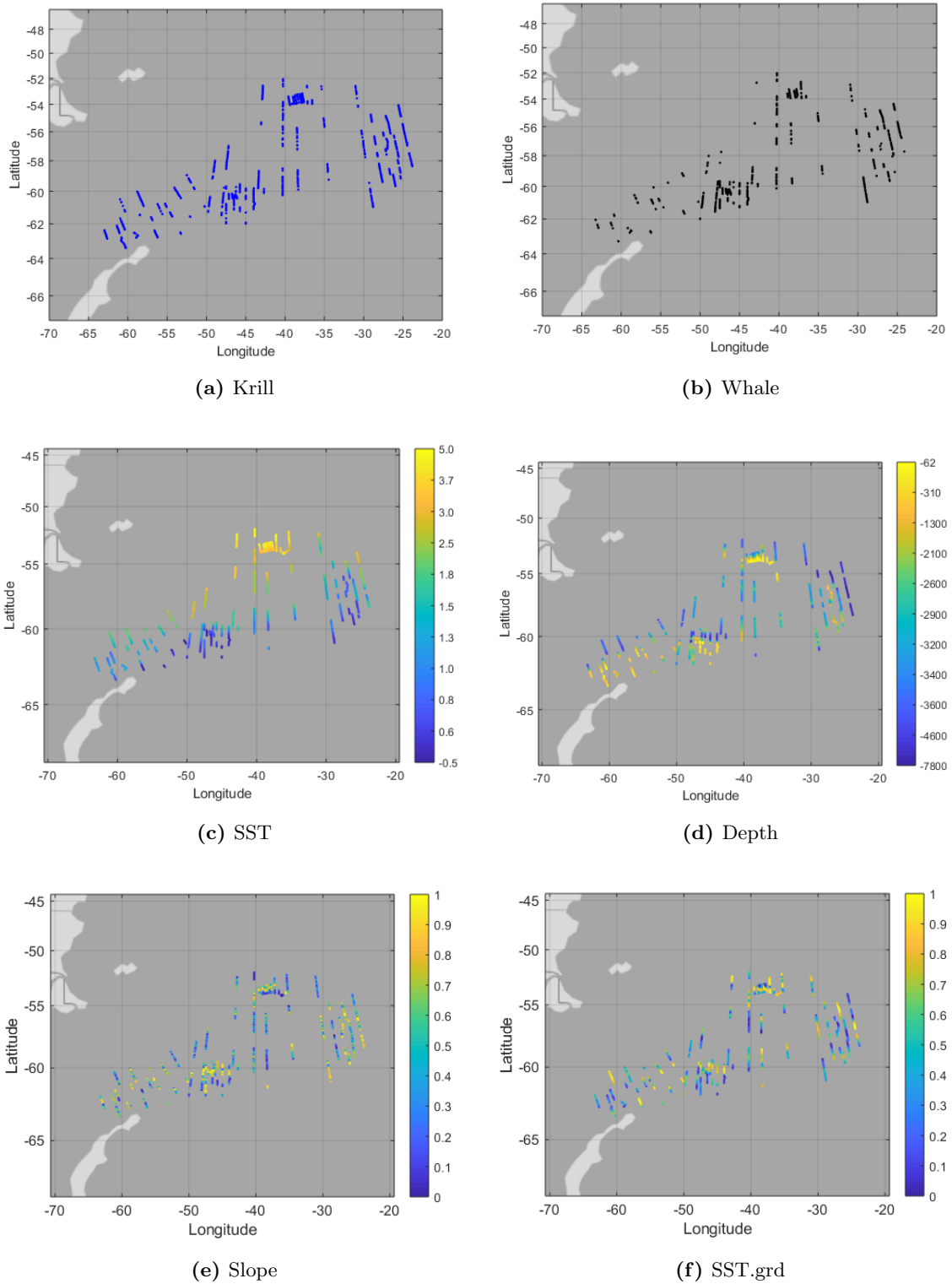


Figure 3: Spatial plots for krill biomass (Krill), sighting data of fin whales (Whale), surface temperature (SST), depth data (Depth), slope for the depth (Slope), and gradient surface temperature (SST.grd).

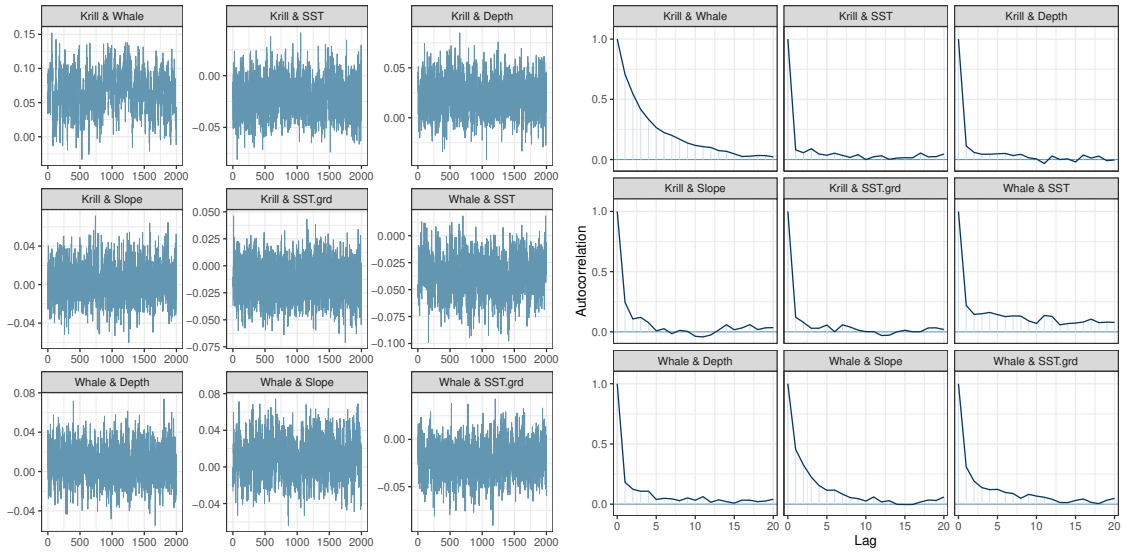


Figure 4: Trace plots and autocorrelation of posterior draws of the correlation coefficients based on our spBGC algorithm.

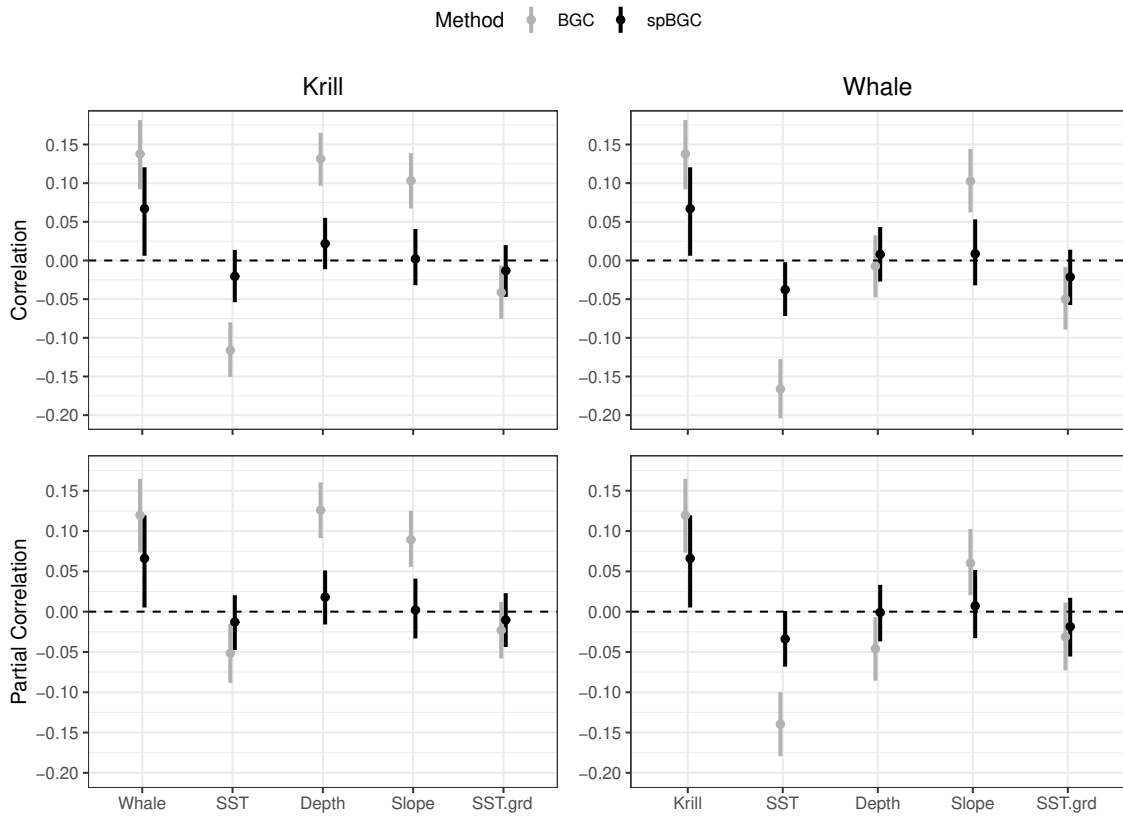


Figure 5: 95% credible intervals with posterior medians (•) of the correlation coefficients (upper) and partial correlations (bottom) based on the proposed method, spBGC, and Hoff (2007)'s one, BGC (grey).

Table 2: 2.5%, 50%, and 97.5% posterior quantiles of the correlation coefficients and partial correlations based on the proposed method, spBGC.

(a) Krill				(b) Whale			
	2.5%	median	97.5%		2.5%	median	97.5%
Correlation				Correlation			
Whale	0.0061	0.0670	0.1205	Krill	0.0061	0.0670	0.1205
SST	-0.0540	-0.0205	0.0137	SST	-0.0718	-0.0378	-0.0022
Depth	-0.0112	0.0218	0.0552	Depth	-0.0273	0.0080	0.0432
Slope	-0.0320	0.0021	0.0407	Slope	-0.0321	0.0087	0.0532
SST.grd	-0.0471	-0.0132	0.0198	SST.grd	-0.0576	-0.0213	0.0140
Partial Correlation				Partial Correlation			
Whale	0.0052	0.0661	0.1196	Krill	0.0052	0.0661	0.1196
SST	-0.0477	-0.0129	0.0204	SST	-0.0682	-0.0339	0.0008
Depth	-0.0159	0.0180	0.0512	Depth	-0.0369	-0.0010	0.0332
Slope	-0.0332	0.0021	0.0410	Slope	-0.0329	0.0071	0.0518
SST.grd	-0.0439	-0.0103	0.0229	SST.grd	-0.0557	-0.0185	0.0172

Table 3: 2.5%, 50%, and 97.5% posterior quantiles of the correlation coefficients and partial correlations based on the method of Hoff (2007), BGC.

(a) Krill				(b) Whale			
	2.5%	median	97.5%		2.5%	median	97.5%
Correlation				Correlation			
Whale	0.0921	0.1378	0.1816	Krill	0.0921	0.1378	0.1816
SST	-0.1506	-0.1161	-0.0800	SST	-0.2041	-0.1662	-0.1275
Depth	0.0966	0.1315	0.1650	Depth	-0.0476	-0.0072	0.0325
Slope	0.0673	0.1033	0.1389	Slope	0.0623	0.1025	0.1442
SST.grd	-0.0754	-0.0412	-0.0065	SST.grd	-0.0894	-0.0501	-0.0086
Partial Correlation				Partial Correlation			
Whale	0.0732	0.1197	0.1648	Krill	0.0732	0.1197	0.1648
SST	-0.0883	-0.0516	-0.0151	SST	-0.1794	-0.1397	-0.0997
Depth	0.0914	0.1261	0.1604	Depth	-0.0856	-0.0459	-0.0068
Slope	0.0556	0.0894	0.1252	Slope	0.0204	0.0602	0.1025
SST.grd	-0.0581	-0.0231	0.0122	SST.grd	-0.0728	-0.0313	0.0113

6 Concluding remarks

We proposed a new semiparametric Bayesian inference for the dependence structure among spatially correlated mixed outcomes, considering a hierarchical spatial model based on the rank likelihood and a latent Gaussian process. We also provided an efficient posterior

computation algorithm using the nearest-neighbor Gaussian process so that a scalable computation can be realized even under large spatial datasets. We investigated the performance of the proposed method compared with the existing method through simulation study. Our proposed method is found to correctly infer the dependence structure among outcomes by successfully taking into account spatial correlation, while the existing method is not. Remarkably, the performance of our method greatly outperforms the existing method as the spatial correlation becomes stronger. We investigated the differences in the results of applying the proposed and existing methods to a real example collected during an international synoptic krill survey in the Scotia Sea of the Antarctic Peninsula.

Regarding the developed posterior computation in Section 3, it involves sampling from the p -dimensional truncated normal (tMVN) distribution. For scalable posterior computation, the discussion on sampling from tMVN is important. As for sampling from tMVN, the Gibbs sampler, which samples from each conditional univariate truncated normal distribution sequentially, is well known (Geweke, 1991; Kotecha and Djuric, 1999; Damien and Walker, 2001). Others sample directly from tMVN one at a time. The algorithm proposed by Pakman and Paninski (2014) samples from tMVN using the Hamiltonian Markov chain (HMC), but requires tuning to obtain good mixing. Botev (2017) proposed an accept-reject algorithm to sample directly from tMVN. This algorithm is implemented in the R package `TruncatedNormal` (Botev and Belzile, 2021). Souris et al. (2018) proposed an approximate MCMC algorithm for sampling from tMVN using the logit function. This idea can be easily extended by using the probit function, and it is suitable for developing a tractable computation for the latent Gaussian process. We performed simulations to compare our spBGC algorithm with various sampling algorithms from tMVN except for Pakman and Paninski (2014) requiring tuning. As a result, we adopt the algorithm of Botev (2017), which is easier to implement, for sampling from tMVN, since little changed in terms of mixing properties. However, when the number of dimensions exceeds 100, the acceptance probability becomes smaller and the algorithm slows down. In such a case, we should consider using other algorithms such as the algorithm using the probit function for sampling from tMVN.

Our proposed method can be applied or extended in several ways. The first is through the Gaussian process formulation for the latent variables, we can obtain the posterior

predictive distribution of the latent variables in arbitrary spatial locations (including non-sampled locations). Then, using the marginal distribution of each outcome estimated in a parametric or nonparametric way, we can carry out spatial prediction in non-sampled locations. Second, although this paper focuses on the latent Gaussian process, the proposed method may be conceptually extendable to other copula models such as elliptical copulas and skew elliptical copulas (Smith, 2021). For example, if one is interested in the tail dependency of a latent process, it may be better to consider the t-copula model. However, a posterior computation of additional parameters by such copula models may not be tractable. In that case, an MCMC sampler based on the Metropolis Hasting algorithm or further efficient computational algorithms may need to be developed. The third is to extend our method to spatio-temporal data. Some multivariate data may have time information as well as location information. For example, the data applied in the application example were observed in the Southern Ocean at different periods. In the analysis of the dependence structure in such data, it may be necessary to take into account not only spatial but also temporal correlations. To this end, we can consider a hierarchical Bayesian spatio-temporal model based on the rank likelihood. Still, the development of the posterior computation for the model is quite challenging and is therefore a subject for future work. Finally, while the proposed methodology is for point-referenced data, it is possible to develop a similar method to estimate copula for multivariate data observed on a graph.

Acknowledgements

This research was supported by JSPS KAKENHI (grant numbers: 21H00699 and 20H00080).

References

- Banerjee, S., B. P. Carlin, and A. E. Gelfand (2003). *Hierarchical Modeling and Analysis for Spatial Data*. Chapman and Hall/CRC.
- Botev, Z. I. (2017). The normal law under linear restrictions: simulation and estima-

- tion via minimax tilting. *Journal of the Royal Statistical Society Series B: Statistical Methodology* 79(1), 125–148.
- Botev, Z. I. and L. Belzile (2021). Truncatednormal: Truncated multivariate normal and student distributions, r package version 2.2.2.
- Damien, P. and S. G. Walker (2001). Sampling truncated normal, beta, and gamma densities. *Journal of Computational and Graphical Statistics* 10(2), 206–215.
- Datta, A., S. Banerjee, A. O. Finley, and A. E. Gelfand (2016). Hierarchical nearest-neighbor gaussian process models for large geostatistical datasets. *Journal of the American Statistical Association* 111(514), 800–812.
- Dey, D., A. Datta, and S. Banerjee (2022). Graphical gaussian process models for highly multivariate spatial data. *Biometrika* 109(4), 993–1014.
- Feng, C. and C. Dean (2012). Joint analysis of multivariate spatial count and zero-heavy count outcomes using common spatial factor models. *Environmetrics* 23(6), 493–508.
- Geweke, J. (1991). Efficient simulation from the multivariate normal and student-t distributions subject to linear constraints and the evaluation of constraint probabilities. In *Proceedings of 23rd Symposium on the Interface between Computing Science and Statistics*, pp. 571–578. Interface Foundation of North America: Fairfax Station, VA.
- Gong, Y. and R. Huser (2022). Flexible modeling of multivariate spatial extremes. *Spatial Statistics* 52, 100713.
- Heller, G. and J. Qin (2001). Pairwise rank-based likelihood for estimation and inference on the mixture proportion. *Biometrics* 57(3), 813–817.
- Hoff, P. D. (2007). Extending the rank likelihood for semiparametric copula estimation. *The Annals of Applied Statistics* 1(1), 265–283.
- Joe, H. (2014). *Dependence modeling with copulas*. CRC press.
- Jordan, M. (2004). Graphical models. *Statistical science* (1), 140–155.

- Kotecha, J. H. and P. M. Djuric (1999). Gibbs sampling approach for generation of truncated multivariate gaussian random variables. In *1999 IEEE international conference on acoustics, speech, and signal processing. Proceedings. ICASSP99 (Cat. No. 99CH36258)*, Volume 3, pp. 1757–1760. IEEE.
- Krafft, B. A., K. G. Bakkeplass, T. Berge, M. Biuw, J. A. Erices, E. M. Jones, T. Knutsen, R. Kubilius, M. Kvalsund, U. Lindstrøm, et al. (2019). *Report from a krill focused survey with RV Kronprins Haakon and land-based predator work in Antarctica during 2018/2019*. Havforskningsinstituttet.
- Krock, M. L., W. Kleiber, D. Hammerling, and S. Becker (2023). Modeling massive highly-multivariate nonstationary spatial data with the basis graphical lasso. *Journal of Computational and Graphical Statistics* (just-accepted), 1–25.
- Krupskii, P. and M. G. Genton (2019). A copula model for non-gaussian multivariate spatial data. *Journal of Multivariate Analysis* 169, 264–277.
- Krupskii, P., R. Huser, and M. G. Genton (2018). Factor copula models for replicated spatial data. *Journal of the American Statistical Association* 113(521), 467–479.
- Liu, J. S. and Y. N. Wu (1999). Parameter expansion for data augmentation. *Journal of the American Statistical Association* 94(448), 1264–1274.
- Macaulay, G., G. Skaret, T. Knutsen, O. Bergstad, B. Krafft, S. Fielding, et al. (2019). Biomass results from the international synoptic krill survey in area 48, 2019. *CCAMLR, SG-ASAM-2019/08*.
- Manly, B. F. and J. A. N. Alberto (2016). *Multivariate statistical methods: a primer*. Chapman and Hall/CRC.
- Mann, K. H. and J. R. Lazier (2005). *Dynamics of marine ecosystems: biological-physical interactions in the oceans*. John Wiley & Sons.
- Musafer, G. N., M. H. Thompson, R. C. Wolff, and E. Kozan (2017). Nonlinear multivariate spatial modeling using nlpca and pair-copulas. *Geographical Analysis* 49(4), 409–432.

- Øien, N. (1995). Norwegian independent line transect survey 1995. *Interne notat* (8-1995).
- Pakman, A. and L. Paninski (2014). Exact hamiltonian monte carlo for truncated multivariate gaussians. *Journal of Computational and Graphical Statistics* 23(2), 518–542.
- Pettitt, A. N. (1982). Inference for the linear model using a likelihood based on ranks. *Journal of the Royal Statistical Society: Series B (Methodological)* 44(2), 234–243.
- Smith, M. S. (2021). Implicit copulas: An overview. *Econometrics and Statistics*.
- Souris, A., A. Bhattacharya, and D. Pati (2018). The soft multivariate truncated normal distribution with applications to bayesian constrained estimation. *arXiv preprint arXiv:1807.09155*.
- Tett, P., R. Gowen, S. Painting, M. Elliott, R. Forster, D. Mills, E. Bresnan, E. Capuzzo, T. Fernandes, J. Foden, et al. (2013). Framework for understanding marine ecosystem health. *Marine Ecology Progress Series* 494, 1–27.
- Torabi, M. (2014). Spatial generalized linear mixed models with multivariate car models for areal data. *Spatial Statistics* 10, 12–26.